Electrochemical and Solid-State Letters, **7** (7) A212-A215 (2004)
0013-4651/2004/7(7)/A212/4/$7.00 © The Electrochemical Society, Inc.

Metal Borides: Competitive High Capacity Anode Materials for Aqueous Primary Batteries

H. X. Yang,[z] Y. D. Wang, X. P. Ai, and C. S. Cha

Department of Chemistry, Wuhan University, Wuhan 430072, China

Experimental results indicated that transition metal borides VB_2 and TiB_2 electrodes can deliver exceptionally high discharge capacity of over 3100 and 1600 mAh/g, respectively, corresponding to an 11 and 6 electron oxidation reaction, although their parent elements V, Ti, and boron, are almost completely electrochemically inert. The reasons for the observed extraordinary capacities of diborides are probably due to the electrochemical activation of boron, which alleviates the passivation of the transition metal by clamping the electrode potential to a less positive range of potential.
 [DOI: 10.1149/1.1753251]

Manuscript submitted July 4, 2003; revised manuscript received October 27, 2003. Available electronically May 12, 2004.

Electrochemical batteries have been serving as convenient power sources for various portable electronic devices. Among the different types of aqueous primary batteries available on the market, the Zn-MnO_2 system has been possessing a dominant share for over a century because of its appropriate performance and low cost. However, despite that the performances of the Zn-MnO_2 have been significantly improved during past decades,[1,2] it seems increasingly difficult for this battery system to satisfy the demands of portable digital devices popping up one after another nowadays. Therefore, the search for new battery systems with higher energy density has always been highlighted in recent decades.[3,4] Nevertheless, metallic zinc (theoretical discharge capacity 820 mAh/g) is still employed predominantly as anode material in almost all aqueous primary systems, including the Zn-NiOOH system recently suggested by Toshiba.[5]

Judging from thermodynamic data,[6,7] many transition metals (TM), such as Ti, V, Mn, and Fe, and nonmetal elements such as B, C, and Si should be capable of performing as competitive high-energy anode materials for aqueous batteries. However, apparently due to their chemical instability or surface passivation, electrodes made from these elements were not capable of delivering their electrochemical capacities in aqueous solutions.

Many intermetallic compounds and metal borides, carbides, and silicides of the TM have thermodynamic parameters and electronic conductivities similar to those of the corresponding TM. Therefore, from the viewpoint of electrochemical energy conversion, these compounds may constitute a large class of promising electrochemically active materials for batteries. The use of metal borides as anode material for batteries has been mentioned by Millennium Cell in the patent literatures.[8] However, to the knowledge of authors of this paper, no experimental result has ever been published. Here we report the preliminary results of experimental study of the electrochemical behavior of TiB_2 and VB_2, to demonstrate the feasibility of using these compounds as high capacity anode materials in aqueous primary batteries.

Experimental

The VB_2 (TiB_2) electrodes are composed of 85% VB_2 (TiB_2) (Aldrich powder, 325 mesh), 8% acetylene black, and 7% polytetrafluoroethylene. The boride electrodes were prepared first by mixing the electrode constituents to form a paste, then roll-pressing the paste to 0.15 mm thick films, and finally pressing the film onto a nickel net. The electrochemical measurements were performed in a three-electrode cell using a small piece (9 mm^2) of the boride electrodes as working electrodes, a large area air cathode as counter electrode, and Hg/HgO as reference electrode. This preparation method of air electrode is similar to those described in Ref. 9 and 10. The air electrodes consist of a catalyst layer and a gas diffusion layer. The catalyst layer is a membrane 0.1 mm thick containing the MnO_2 catalyst (20 wt %) loaded on activated carbon (65 wt %) and polytetrafluoroethylene binder (15 wt %). The gas diffusion layer was prepared by mixing acetylene black (60 wt %) and PTFE emulsion (40 wt %) with isopropanol to form a paste and then rolling the paste to 0.5 mm thick film. Both layers were pressed together with a nickel mesh in between at 80 kg/cm^2 and sintered at 270°C in air for half an hour to remove organic residues.

To calculate quantitatively the electric charges generated in the electro-oxidation of the diboride electrodes, the cyclic voltammograms (CVs) of the metal boride electrodes were recorded at a very slow sweep rate ($0.05\ mV\ s^{-1}$) to avoid the possible distortions from sluggish kinetics of the electrode reactions. The electrochemical discharge capacities of the boride electrodes were also evaluated by galvanostatic discharge experiments in the laboratory cells using 4 cm^2 VB_2 (TiB_2) electrode as anode, 25 cm^2 air electrode as inexhaustible cathode, and 30% KOH solution as electrolyte.

The discharge reaction products of the boride electrodes were analyzed by colorimetric determination of titanate ions and vanadate ions according to procedures described in Ref. 11. The qualitative identification of TiO_3^{-2} ions as a soluble discharge product of TiB_2 electrode was based on the appearance of a yellow color after adding 3% $H_2\ O_2$ into the acidified cell electrolyte, and the quantitative determination of the Ti content was made by absorbance analysis at 420 μm using a spectrophotometer (721 type, Shanghai Analytical Instrument Corp., China). Similarly, VO_3^{-1} ions in the electrolyte were identified by the reddish brown color produced by the reaction of pentavalent vandium with hydrogen peroxide in acidified electrolyte and quantitatively determined by spectrophotometric analysis. The qualitative and quantitative determination of boron in electrolyte was also made by spectrophotometric measurement based on the color change of carminic acid from red to bluish tint in sulfuric acid in the presence of boron. The quantitative determination of the titanium and boron content were also carried out by inductively coupled plasma (ICP) spectrometry.

The solid phases of both TiB_2 and VB_2 electrodes before and after discharge were examined by X-ray diffraction (XRD) using a Shimadzu lab XRD diffractometer with Cu Kα source.

Results and Discussion

Figure 1 depicts the CVs obtained with TiB_2 and VB_2 powder electrodes in 30% KOH solution. A common feature of these CV curves is the appearance of well-defined current peaks on the anodic branches. From the weight of metal boride and the area of these peaks it can be calculated that the electric quantity released from the anodic oxidation of TiB_2 powder is *ca.* 2200 mAh/g, which is near the theoretical $6e^-$ oxidation capacity of 2314 mAh/g; and the discharge capacity of VB_2 powder is about 4100 mAh/g, which is near the theoretical $11e^-$ oxidation capacity of 4063 mAh/g.

To test the practical feasibility of employing the metal diboride electrodes as high capacity anodic materials, we constructed simulated diboride air cells and discharged the cells at relatively high

[z] E-mail: ece@whu.edu.cn

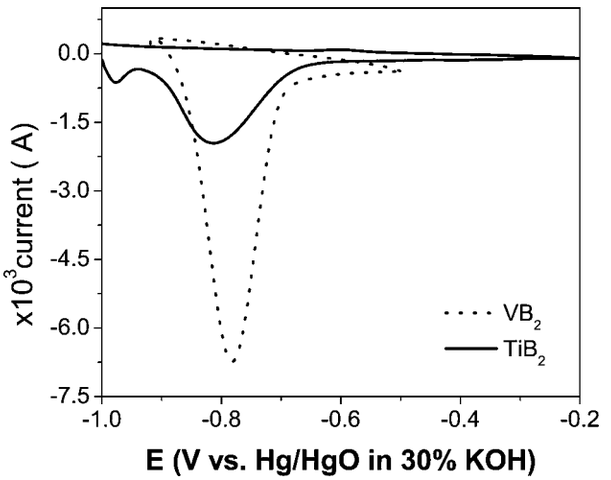

Figure 1. CVs of TiB_2 (2.6 mg) and VB_2 (2.1 mg) electrodes in a 30% KOH solution. Potential sweep rate was set at 0.05 mV/s.

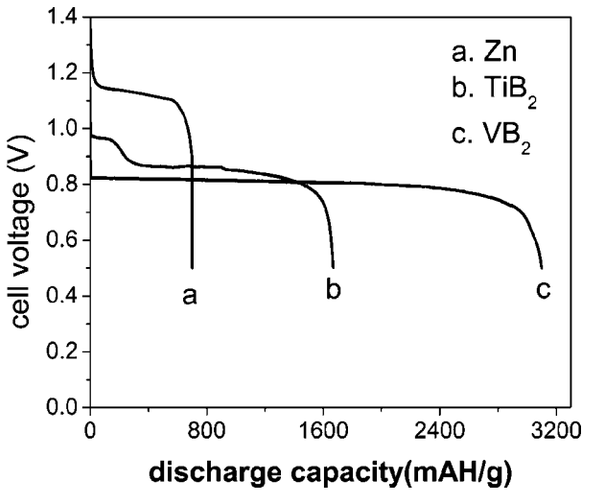

Figure 3. A comparison of the discharged capacities of VB_2 and TiB_2 with Zn powder electrode. All cells were constructed using air cathodes and discharged at 100 mA/g.

current densities. Figure 2 shows the discharge curves of TiB_2 and VB_2 powder electrodes. It is clear from the figure that the practically attainable discharge capacity of VB_2 powder electrode may be over 3100 mAh/g at 100 mA/g and *ca.* 2900 mAh/g at a very high discharge rate of 500 mA/g. These values are three to four times higher than the theoretical discharge capacity of Zn, and, to our knowledge, are the highest discharge capacity values for solid electroactive materials ever reported in the literature. These values also indicate that the VB_2 powder electrode can serve not only as ''high energy density anode,'' but also as ''high power density anode.'' The TiB_2 powder electrode can achieve *ca.* 1600 mA/g at 100 mA/g and 900 mAh/g at 500 mA/g, respectively; also well above the theoretical discharge capacity of metallic zinc anode. In Fig. 3 the discharge curves of TiB_2, VB_2, and Zn electrodes are compared to demonstrate the superior behavior of the transition metal boride electrodes. However, the plateau on the discharge curves of TM boride electrodes is about 0.3 V lower than that of the Zn electrode.

To elucidate the reaction mechanisms of the diboride electrodes, it is of primary importance to find out the discharge products, including both solid phase products and products soluble in the electrolyte. Figure 4 shows the XRD patterns of a VB_2 electrode before and after discharge. It is clear from Fig. 4 that after discharge the original XRD lines of VB_2 fade out almost completely and no XRD signals from new crystalline phases are evident, implying that the discharge products of VB_2 are probably completely dissolved in electrolyte solution. By spectrophotomeric analysis of the electrolyte, we found that the discharge products of the VB_2 electrode exist mainly in the forms of BO_3^{3-} and VO_4^{3+} in electrolyte and the amounts of BO_3^{3-} and VO_4^{3+} formed in electrolyte are in accordance with the $11e^-$ electrochemical oxidation reaction mechanism. Table I compares the discharged capacities of the VB_2 and TiB_2 electrode with the capacity values calculated from the amounts of VO_4^{3+}, Ti^{4+}, and BO_3^{3-} ions found in electrolyte after discharge. Clearly, the experimental discharge capacity of the VB_2 electrode agrees well with the capacity value calculated from the amounts of VO_4^{3+} and BO_3^{3-} formed in electrolyte, suggesting that the oxidation reaction of the VB_2 electrode seems to proceed according to the following mechanism

$$VB_2 + 20\ OH^- \rightarrow VO_4^{3-} + 2\ BO_3^{3-} + 10H_2O + 11e^- \quad [1]$$

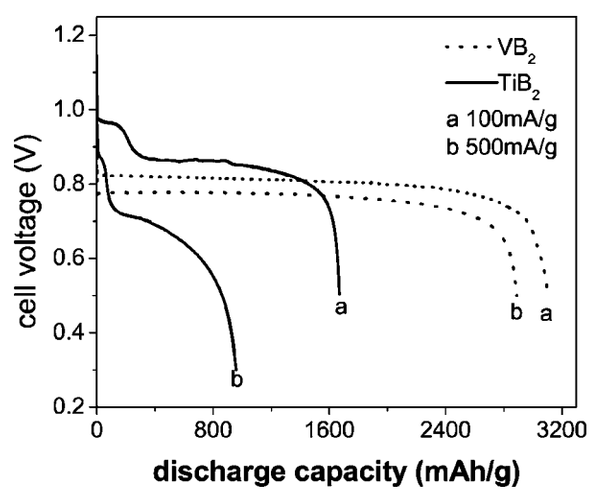

Figure 2. Discharge curves of (· · · ·) VB_2 and (——) TiB_2 electrodes in a 30% KOH solution at constant current of (a) 100 and (b) 500 mA/g. The voltage profiles were recorded as E(air cathode) − E(metal boride).

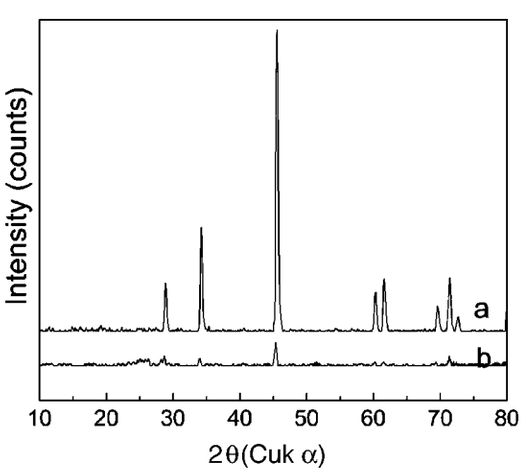

Figure 4. XRD patterns of VB_2 anodes: (a) before discharge and (b) after complete discharge to 0.5 V.

Table I. Comparison of the experimental discharged capacities of the VB_2 and TiB_2 electrode with the capacity values calculated from the amounts of VO_4^{3+}, Ti^{4+}, and BO_3^{3-} ions dissolved in the discharged electrolyte.

		Discharge product in electrolyte (amount/theoretical capacity)			
	C_{exp}[a] (mAH)	BO_3^{3-} (mg/mAH)	Ti^{4+} (mg/mAH)	VO_4^{3-} (mg/mAH)	C_{cal} (mAH)
TiB_2	112.9	72.8/99.5	4.9/10.9	—	110.4
VB_2	291.7	173.2/236.8	—	156.2/182.1	418.9

[a] C_{exp} denotes the discharge capacity measured from experimental cell. C_{cal} denotes the sum of theoretical capacity calculated from the amount of BO_3^{3-}, Ti^{4+}, and VO_4^{3-} found in electrolyte. $6e^-$ and $11e^-$ oxidation mechanisms are assumed for TiB_2 and VB_2 electrodes, respectively, in the calculation of theoretical capacity.

However, the discharge behaviors of TiB_2 electrode are more difficult to understand. First, on the discharge curves of TiB_2 electrode in Fig. 2 a small step (corresponding to the discharge of less than one electron per TiB_2) appears before the main discharge plateau. On the anodic branch of CV curve of TiB_2 shown in Fig. 1, a small peak is also visible before the main peak. The mechanism responsible for this small step and small peak is still not clear. Second, it can be seen from Table I that only a relatively small amount of Ti^{4+} was found in electrolyte (corresponding to less than 10% discharge capacity). From results of spectroscopic analysis of the electrode, it was found that the major part of Ti is still in the electrode after discharge. XRD analysis of the fully discharged TiB_2 electrode (Fig. 5) revealed that the XRD peaks due to TiB_2 decreased significantly, but no new crystalline phase was observed. Nevertheless, electron probe microanalysis of the TiB_2 anodes indicated that the Ti content in the discharged electrode was almost the same as in a freshly prepared electrode. A probable mechanism is that Ti exists in the discharged electrode as amorphous titanium, which is formed after the electrochemical leach out of boron.

After complete discharge of the TiB_2 electrode, BO_3^{3-} was identified as the only major discharge product in electrolyte, and its amount was almost quantitatively (>95%) in accordance with the $6e^-$ oxidation mechanism (Table I). Therefore the principal discharge reaction of the TiB_2 electrode oxidation seems to be

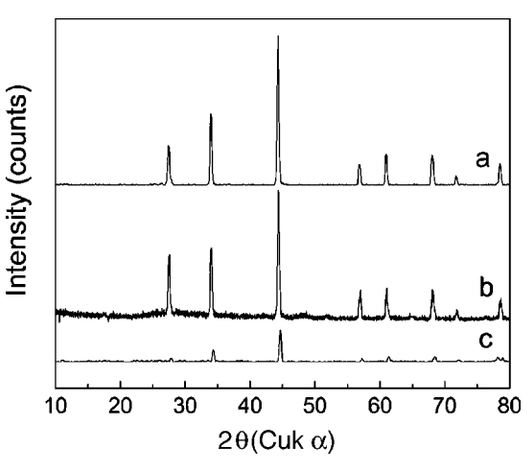

Figure 5. XRD patterns of TiB_2 anode: (a) before discharge, (b) after discharge to the stage corresponding to the completion of first potential step, and (c) after complete discharge to 0.5 V.

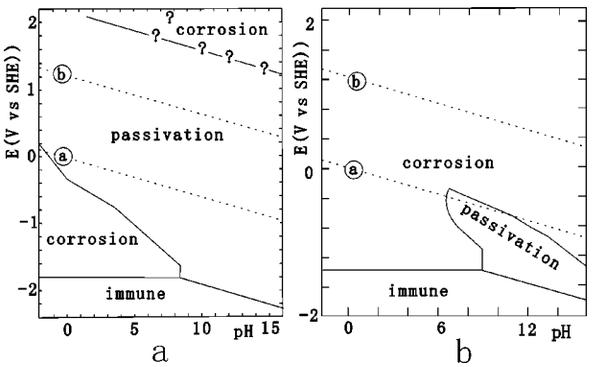

Figure 6. pH-potential diagram for (a) Ti and (b) V, schematically reconstructed from data shown in Ref. 14.

$$TiB_2 + 12\ OH^- \rightarrow 2\ BO_3^{3-} + Ti(\text{amorphous}) + 6H_2O + 6e^- \quad [2]$$

The above-stated results clearly indicate that boron in both TiB_2 and VB_2 is electrochemically very active in 30% KOH solution, in contrast with the behavior of elementary boron electrode, which is almost completely inert in alkaline solutions. It is really impressive to find out that TiB_2 and VB_2, both well known for their very high chemical stability, could react so energetically as anode materials for batteries. However, the observed anodic reaction of boron oxidation takes place in a potential range far more positive than the theoretical equilibrium potential (about −1.8 V, *vs.* a standard hydrogen electrode (SHE), as calculated from thermodynamic data) of these electrodes. The observed anodic reactions were realized under a condition of very high overpotential (*ca.* 1 V, *i.e.*, the reactions are highly irreversible).

At the present stage, we are still unable to ascertain whether the observed different behavior between the boron electrode and TM boride electrodes is due to the difference of structure of surface oxides or differences of some other parameters (such as electronic conductivity, electron work function, etc.). The crystalline structure of TM diborides is simply a hexagonal lattice consisting of closely packed TM layer and graphite-like B layer alternately.[12] Unlike most layered compounds, there exist strong interlayer interactions between the TM layer and B layer. Previous studies of the electronic structure and bonding of MB_2-type TM diborides have revealed that there are at least three types of bondings present in MB_2 compounds: The bonding between TM atoms is dominantly of a metallic nature, while the bonding between boron atoms is covalent sp^2 hybrid. The TM and B atoms are bonded by a finite ionic bond through electron donation from the TM atoms to B atoms.[13] Because the hybrid bonding between the TM and B atoms and between B atoms are not as strong as the covalent sp^2 hybrid bonding of B-B atoms in solid boron, the chemical stability of the B atoms is weakened, so the electrochemical liberation of electrons from the B atoms should be facilitated in the TM diborides.

The next question would be why TiB_2 and VB_2 electrodes behave so differently in discharge reaction. Examination of the pH-potential diagrams for Ti and V, which are depicted schematically in Fig. 6a and b (original diagrams can be found in Ref. 14), seems to provide some hints to the solution of this question. Figure 6b shows that, in solution of pH 15, the vanadium electrode is passive at the potential of equilibrium, but electrochemically active (anodic dissolution highly probable) in the potential range of boron oxidation (around −0.7 V *vs.* SHE, which is *ca.* 0.1 V lower than a Hg/HgO reference electrode). Therefore, vanadium could oxidize together with boron to complete an $11e^-$ reaction as shown in Eq. 1. From the pH-potential diagram for Ti (Fig. 6a), it is clear that the Ti electrode surface remains in the passivated state in pH 15 solution in

a potential range around −0.7 V *vs.* SHE, so we should not expect that Ti could oxidize together with boron during the discharge of the TiB_2 electrode.

The above-stated experimental results and discussion seem to indicate clearly that boron in TM diborides may serve as a very high discharge capacity and high power density anode for primary aqueous batteries. The TM element in TM diboride may also discharge as active anode if the metal is electroactive in a potential range of boron oxidation as in the VB_2 electrode. If the TM is in the passivated state in a potential range of boron oxidation, it probably will not take part in the discharge reaction as in the TiB_2 electrode.

Acknowledgment

The authors gratefully acknowledge financial support by the 973 Program, China (grant no. 2002CB211800).

Author H. X. Yang assisted in meeting the publication costs of this article.

References

1. R. M. Dell, *Solid State Ionics*, **134**, 140 (2000).
2. C. C. Yang and S. J. Lin, *J. Power Sources*, **112**, 174 (2002).
3. S. Licht, S. Ghosh, and V. Naschitz, *Electrochem. Solid-State Lett.*, **4**, A209 (2001).
4. S. Licht, B. Wang, and S. Ghosh, *Science*, **285**, 1039 (1999).
5. http://gigaenergy.toshiba.com/ecoming.html
6. W. M. Latimer, *The Oxidation State of the Elements and Their Potentials in Aqueous Solutions*, 2nd ed., Prentice-Hall, New York (1952).
7. A. J. Bard, R. Parsons, and J. Jordan, *Standard Potentials in Aqueous Solutions*, Marcel Dekker, New York (1985).
8. S. Amendola, U. S. Pat. 5,948,558 (1999); S. Amendola, U. S. Pat. 6,468,694 (2002).
9. S. Muller, F. Holzer, H. Arai, and O. Haas, *J. New Mater. Electrochem. Syst.*, **2**, 227 (1999).
10. S. Muller, K. Striebel, and O. Haas, *Electrochim. Acta*, **39**, 1661 (1994).
11. N. H. Furman, *Standard Methods of Chemical Analysis*, Vol. 1, 6th ed. Chap. 48 and 51, D. Van Nostrand Company Inc., Princeton, NJ (1962).
12. T. P. Fehlner, *J. Solid State Chem.*, **154**, 110 (2000).
13. P. Vajeeston, P. Ravindran, C. Ravi, and R. Asokamani, *Phys. Rev. B*, **63**, 045115 (2001).
14. M. Pourbaix, *Atlas d'Equilibres Electrochimiques*, p. 219, 243, Gauthier-Villars, Paris (1963).